



Muon density spectra as a probe of the muon component predicted by air shower simulations

A. Haungs^{a*}, T. Antoni^b, W.D. Apel^a, F. Badea^{b†}, K. Bekk^a, A. Bercuci^{a†}, H. Blümer^{a,b}, H. Bozdog^a, I.M. Brancus^c, C. Büttner^a, A. Chilingarian^d, K. Daumiller^b, P. Doll^a, J. Engler^a, F. Feßler^a, H.J. Gils^a, R. Glasstetter^b, R. Haeusler^b, D. Heck^a, J.R. Hörandel^b, A. Iwan^{b‡}, K.-H. Kampert^{b,a}, H.O. Klages^a, G. Maier^a, H.J. Mathes^a, H.J. Mayer^a, J. Milke^a, M. Müller^a, R. Obenland^a, J. Oehlschläger^a, S. Ostapchenko^{b§}, M. Petcu^c, H. Rebel^a, M. Risse^a, M. Roth^a, G. Schatz^a, H. Schieler^a, J. Scholz^a, T. Thouw^a, H. Ulrich^b, J.H. Weber^b, A. Weindl^a, J. Wentz^a, J. Wochele^a, J. Zabierowski^e

^aInstitut für Kernphysik, Forschungszentrum Karlsruhe, 76021 Karlsruhe, Germany

^bInstitut für Experimentelle Kernphysik, Universität Karlsruhe, 76021 Karlsruhe, Germany

^cNational Institute of Physics and Nuclear Engineering, 7690 Bucharest, Romania

^dCosmic Ray Division, Yerevan Physics Institute, Yerevan 36, Armenia

^eSoltan Institute for Nuclear Studies, 90950 Lodz, Poland

The KASCADE experiment measures local muon densities of air-showers in the knee region at various core distances for two different muon energy thresholds. Muon density spectra have been reconstructed for the total EAS sample, as well as for particular subsamples with enhanced light and heavy induced EAS, classified on the basis of the shower size ratio N_μ/N_e . By comparing these spectra for different muon energy detection thresholds and core distances with detailed Monte Carlo simulations each spectrum should result in the same primary energy spectrum. This allows a comprehensive test of the simulation procedures of the muon lateral distribution and the muon energy spectrum by various Monte Carlo codes. Different combinations of high-energy and low-energy interaction models in the frame of the CORSIKA code are used for comparisons.

1. Introduction

Frequency spectra of the extensive air-shower (EAS) observables (like number of electrons or charged particles) reflect the primary energy spectrum, but a quantitative conversion to energy has to invoke a model of the shower development and an assumption of a mass composition [1]. Hence the determination of the energy spectrum is affected by different systematic uncertainties, especially by the dependence on the model of high-energy interactions. Therefore the validity of the hadronic interaction models used as generators of Monte Carlo simulations is an important subject in context of EAS analyses. Here a co-operation between present and future accel-

erator experiments and the cosmic ray investigations is aspired [2], but also by cosmic ray measurements there appear possibilities to probe the validity of the models [3,4]. It is useful to analyze different experiments on basis of a coherent methodology as well as to compare the resulting features for various sets of different EAS parameters in the individual experiments.

In the present paper we endeavor to analyze the frequency distribution of local muon densities at fixed distances from the shower core. Thus independent measurements of such spectra for different fixed core distances allow a check of the lateral distribution obtained from simulations. In addition, the layout of the KASCADE experiment [5] enables the study of density spectra for two different muon energy thresholds. Hence the consistency of the simulations with respect to the muon energy spectrum and systematic features of different models can be revealed.

*corresponding author, e-mail: andreas.haungs@ik.fzk.de

†on leave of absence from National Institute of Physics and Nuclear Engineering, Bucharest, Romania

‡on leave of absence from University of Lodz, Poland

§on leave of absence from Moscow State University Moscow, Russia

2. Local muon density spectra

The main detector components of KASCADE used for the present analysis are the “array” of 252 stations and the “central detector” comprising additional detector systems. The array provides the data necessary for the reconstruction of the basic EAS characteristics like electron and muon size, core location, and arrival direction of individual air showers [6]. The KASCADE central detector is placed in the geometrical center of the detector array. The local muon density of the EAS is measured with two separate detector set-ups. A setup of 32 large multiwire proportional chambers (MWPC) [7] is installed in the basement of the building and enables the estimation of the muon density ρ_μ^* for each single EAS. The total absorber corresponds to a threshold for muons of 2.4 GeV. The second muon detection system is a layer of 456 plastic scintillation detectors in the third gap of the central detector, called trigger plane [8]. Here the muon density ρ_μ^{tp} is estimated for muons with a threshold of 490 MeV for vertical incidence. The total sample of EAS is further divided in “electron-rich” and “electron-poor” showers performed by a cut along the ratio $\lg(N_\mu)/\lg(N_e)$, i.e. observables estimated by the array data only. The reconstruction of muon density spectra of all samples have been performed for both energy thresholds and for nine core distance ranges [9]. For the fit procedure the flux $\lg(dN/d\rho_\mu)$ is assumed to follow a power law below and above a specified knee region. As example Fig. 1 shows the reconstructed local muon density spectra for the average distance from the shower axis $\langle R_c \rangle = 45.5$ m for both muon energy thresholds. Spectra for all, for the electron-rich (predominantly light ion induced), and for the electron-poor (predominantly heavy ion induced) showers are displayed. The general features of the spectra are similar for all core distance ranges; the all-particle spectra show a slight, but significant kink, the component of electron-rich EAS dominates the flux below the knee while it strongly decreases after the kink, and no knee is seen in the component of electron-poor EAS. Whereas the assumed fit functions describe the all-particle spectra well, the spectra

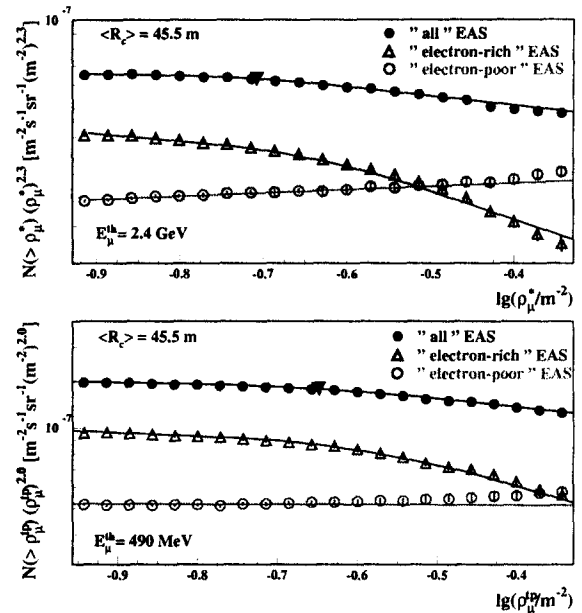


Figure 1. Examples for measured muon density spectra for both threshold energies. The “all”-particle spectra are here compared with the spectra of “electron-poor” and “electron-rich” EAS for the same core distance range.

for the electron-rich subsamples are not well described by power-laws above the knee position in the all-particle spectra. These pure experimental results are a strong indication that the knee in the primary cosmic ray spectrum originates from a cut-off in the flux of the light primary particles.

3. Comparisons with simulations

For the interpretation of the measured muon density spectra in terms of the primary energy spectrum a-priori knowledge inferred from Monte Carlo simulations of the air-shower development is necessary. The present analysis is based on a large set of CORSIKA simulations [10] including a full simulation of the detector response. The simulations have been performed using the interaction models QGSJET (vers. of 1998 [11]), SIBYLL (vers.2.1 [12]), and NEXUS (vers.2 [13]) for the high-energy interactions and

GHEISHA [14] and UrQMD [15] for interactions below $E_{\text{lab}} = 80$ GeV. The electromagnetic part of the showers is treated by EGS4 [16]. Observation level, Earth's magnetic field, and the particle thresholds are chosen in accordance with the experimental situation of KASCADE. The simulations cover the energy range of $10^{14} - 3 \cdot 10^{16}$ eV. The calculations are performed for the zenith angular range $0^\circ - 42^\circ$ and for three primary masses: protons, oxygen and iron nuclei.

For a test of the interaction models by comparing the calculated predictions with air shower data the sensitivity to differences in the simulations should be of significance. Fig. 2 shows the relative differences of various model combinations for relevant EAS observables ($\frac{O(\text{qgsjet gheisha}) - O(\text{other models})}{O(\text{qgsjet gheisha})}$) of KASCADE in dependence of the primary energy. While in general all model calculations predict only minor differences in the electron number, the total muon number and especially the predictions of local muon densities differ considerably (up to 20%), increasingly with increasing primary energy.

When relating the measured density spectra to the primary energy spectrum of cosmic rays a power law spectrum $dN/dE_0 \propto E_0^{-\gamma}$ is assumed. The energy spectrum can be written as $(dN/d\rho_\mu) \cdot (d\rho_\mu/dE_0)$, where $d\rho_\mu/dE_0$ has to be deduced from the EAS simulations and $dN/d\rho_\mu \propto (\rho_\mu)^{-\beta}$ is taken from the experimental results. Thus the spectral index γ can be expressed by $\gamma = \delta \cdot (\beta - 1) + 1$ with δ from the simulations ($\rho_\mu \propto E_0^\delta$). If the correct elemental composition is adopted, all measured muon density spectra (of the total sample or of a certain subsample) should result consistently in the true primary energy spectrum, irrespectively which core distance and muon energy threshold is considered.

For all model combinations we found that the muon density spectra for the different core distances agree within their statistical uncertainties for the resulting slopes and knee positions of the primary mass. This corroborates the confidence in the lateral distribution predicted by the Monte Carlo simulations. Nevertheless there remain obvious systematic differences in the results for the two muon energy thresholds, observed for all core

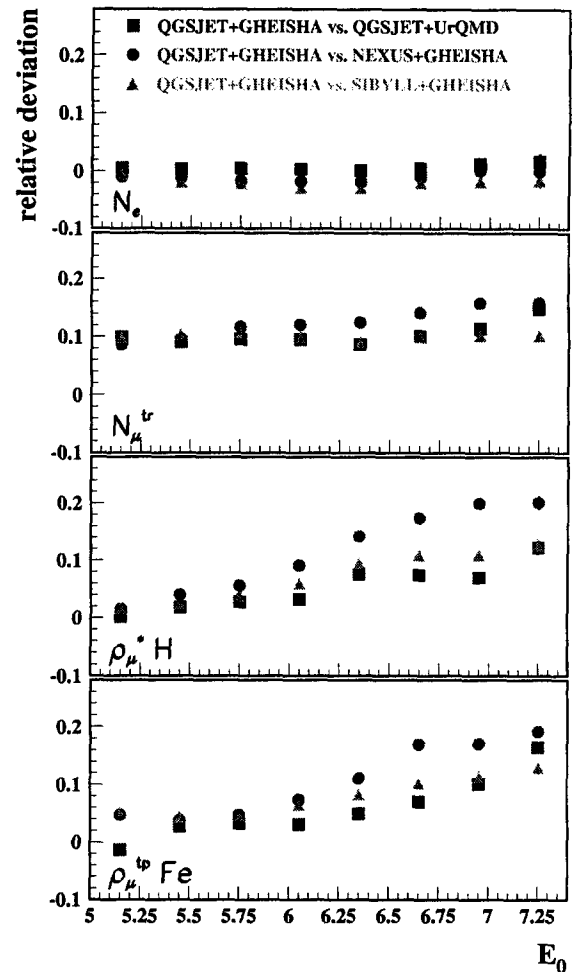


Figure 2. Relative deviations of air-shower observables at KASCADE after full detector simulations for different model combinations. All with respect to the combination QGSJET/GHEISHA.

distances. Fig. 3 displays this observation in case of the spectral index of the electron-poor sample using the simulations of primary iron nuclei. Uncertainties by the unknown composition can not explain the systematic discrepancy displayed by the results from the two different muon energy thresholds. These systematic differences for the two thresholds remain in all spectra, and, more or less for all considered model combinations (Fig. 3). To reduce this systematic shift a

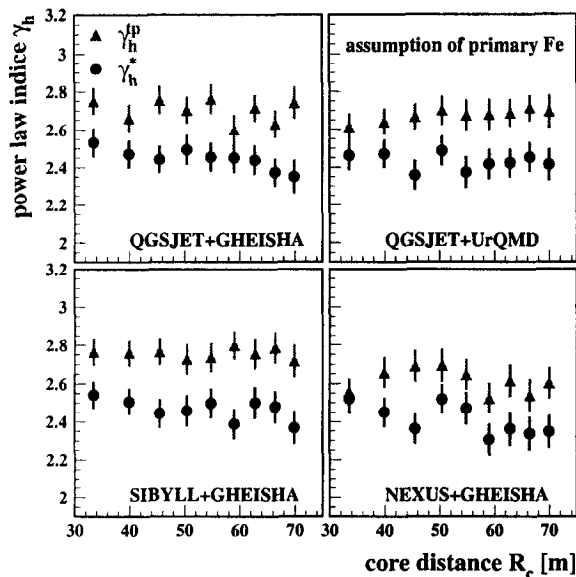


Figure 3. Variation of the reconstructed power law index of the primary energy spectrum (electron-poor sample) with the core distance for both energy thresholds assuming a pure iron composition for different combinations of the interaction models.

model combination predicting a smaller ratio in the number of lower energy muons to high-energy muons with a smaller value of δ in the dependence $\rho_\mu \propto E_0^\delta$ (again more pronounced for the lower muon threshold) is needed. The behaviour of the models NEXUS and UrQMD comply with these requirements better than QGSJET, SIBYLL, or GHEISHA.

4. Conclusions

In conclusion we found that the muon lateral distribution in the models is described sufficiently, with a hint to a better description in the low energy model UrQMD compared to the GHEISHA parameterization. Still none of the investigated model combinations describe consistently the muon fluxes above the two considered energy thresholds, i.e. the muon energy spectrum.

Acknowledgement The KASCADE experiment is supported by collaborative WTZ projects in the frame of the scientific-technical cooperation between Germany and Romania (RUM 97/014), Poland (POL 99/005) and Armenia (ARM 98/002). The Polish group (Soltan Institute and University of Lodz) acknowledges the support by the Polish State Committee for Scientific Research (grant No. 5 P03B 133 20).

REFERENCES

1. A. Haungs, Proc. XIth ECRS, Moscow 2002, to be published in J.Phys.G .
2. See talks at the NEEDS-workshop's webpage: <http://www-ik.fzk.de/~needs/>
3. T. Antoni et al., KASCADE Collaboration, J.Phys.G 25 (1999) 2161.
4. T. Antoni et al., KASCADE Collaboration, J.Phys.G 27 (2001) 1785.
5. H.O. Klages et al., KASCADE collaboration, Nucl. Phys. B (Proc. Suppl.) 52B (1997) 92.
6. T. Antoni et al., KASCADE Collaboration, Astrop.Phys. 14 (2000) 245.
7. H. Bozdog et al., Nucl.Instr.Meth. A465 (2001) 455.
8. J. Engler et al., Nucl.Instr.Meth. A427 (1999) 528.
9. T. Antoni et al., KASCADE Collaboration, Astrop.Phys. 16 (2002) 373.
10. D. Heck et al., FZKA 6019, Forschungszentrum Karlsruhe, 1998.
11. N.N. Kalmykov and S.S. Ostapchenko, Yad. Fiz. 56 (1993) 105.
12. R. Engel, Proc.26th ICRC, HE 2.5.03, 1 (1999) 415.
13. H.J. Drescher et al., Phys. Rep. 350 (2001) 93.
14. H. Fesefeldt, PITHA-85/02, RWTH Aachen, 1985.
15. M. Bleicher et al., J.Phys.G 25 (1999) 1859; S.A. Bass et al., Prog. Part. Nucl. Phys. 41 (1998) 225.
16. W.R. Nelson et al., Report SLAC 265, 1985.